PERGAMON

AE International – Asia

Atmospheric Environment 37 (2003) 4625–4636

ATMOSPHERIC ENVIRONMENT

www.elsevier.com/locate/atmosenv

The soil particle size dependent emission parameterization for an Asian dust (Yellow Sand) observed in Korea in April 2002

Hee-Jin In, Soon-Ung Park*

School of Earth and Environmental Sciences, Seoul National University, San 56-1 Shilim-Dong, Kwanak-Ku, Seoul 151-742, South Korea

Received 3 April 2003; received in revised form 24 July 2003; accepted 30 July 2003

Abstract

Intense Asian dust (Yellow Sand) events have been observed in Korea on 21–23 March and 7–9 April 2002. During these periods the observed PM_{10} concentrations were over $1000\,\mu g\,m^{-3}$ at most monitoring sites in South Korea. The operational meteorological model of the Regional Data Assimilation and Prediction System of the Korea Meteorological Administration and the aerosol transport model with the improved particle size distribution parameterization developed at Seoul National University were used to simulate the intense Yellow Sand event observed on 7–9 April 2002. The comparison with the observational data shows that the present model system could reasonably simulate the evolutionary features of Yellow Sand over South Korea including the starting and ending time of the event, the particle size spectrum and the PM_{10} concentration. It was found that the dominant particle diameter in the mass concentration ranged from 3.67 to 10 μm during this dust event. A promising dust emission model depending on the particle size distribution constructed by the sum of several log-normal distributions of particle sizes of different soil types has been developed and found to yield better spectral-mass concentration in the size range of larger than 10 μm. This result suggests that size distributions of Asian dust (Yellow Sand) are consistent with those found in the USA, Central Asia and the Sahara desert. However, the accuracy of the model requires more detailed soil particle distributions in the source region.

Keywords: Dispersed particle size distribution; Intense Yellow Sand event; Log-normal distribution of soil particle; Regional data assimilation and prediction system; Spectral-mass concentration

1. Introduction

In recent years, the rapid developing desertification that might result from heavy cultivation, overgrazing and lack of precipitation in the northeastern parts of China has caused the increase in intense and more frequent dust storms in East Asia (Bai and Zhang, 2001; Park, 2002). An exceptionally severe Asian dust (called "Yellow Sand" in Korea) event was observed in Korea for the period of 7–8 April 2002. The maximum observed PM_{10} concentration over South Korea exceeded $1000\,\mu g\,m^{-3}$ which is about 10 times higher than that of the non-dust period. This event has caused natural disasters including temporally closing of most of airports and elementary schools in Korea. Thus the quantitative forecast of Asian dusts is imperatively needed for the prevention of hazardous consequences of dust storms.

In and Park (2002a) have simulated a Yellow Sand phenomenon that was observed over Korea for the period of 14–24 April in 1998. They could simulate quite similar spatial distribution patterns of dust compared to those of aerosol index obtained by total ozone mapping spectrometer (TOMS). However, the simulated dust concentration underestimated the observed total suspended particulate (TSP) concentration in South Korea. This discrepancy might be caused by inaccurate

*Corresponding author. Tel./fax: +82-2-880-6715.
E-mail address: supark@snupbl.snu.ac.kr (S.-U. Park).

1352-2310/$ - see front matter
doi:10.1016/j.atmosenv.2003.07.009

delineation of source regions and emission amounts estimated by the threshold friction velocity that was based on the results of Westphal et al. (1987) and Gillette (1981). Recently, Park and In (2003a, b) modified the dust emission mechanism used in In and Park (2002a) by using statistical analysis of the World Meteorological Organization (WMO) synoptic reporting data for 7 years from 1996 to 2002 in the source regions and employed to simulate long-range transport of an intense Yellow Sand event observed during 21–22 March 2002 in Korea. The simulation showed much improved results in terms of temporal and spatial distribution of dust concentration, starting and ending times of the Yellow Sand event over the Korean peninsula.

Emitted particles in dust source regions have a wide range of size distributions. Park and In (2003a, b) have elaborated dust emission conditions in the source region. However, they have employed the emitted particle size distribution of Westphal et al. (1987, 1988). Namely, the spectral-mass flux of the aerosol is proportional to the power of 1.5 of the particle radius

$$\frac{\mathrm{d}F_a}{\mathrm{d}\log r} \propto r^{1.5}, \tag{1}$$

where F_a is the dust flux from the surface and r the radius of the dust particle. The spectral-mass concentration pattern of the model using Eq. (1) yields quite different pattern compared to the measurement in South Korea. Eq. (1) predicts a significant high concentration in the range of 10–25 μm. During the Asian dust period in April 1998, size-separated number concentrations of aerosols at Seoul and Anmyondo in Korea (Fig. 1) showed a significant increase in the size range of 1.35–10 μm (Chun et al., 2001a), that is, observed common features during the Asian dust periods in the Korean peninsula.

An additive form of several log-normal size distributions for soils is proposed to estimate emission amount in many studies (Gomes et al., 1990; Chatenet et al., 1996; Shao, 2001; Shao et al., 2002) without observational evidence in Northeast Asia. This study is mainly focused on the development of the particle size dependent emission parameterization for a dust event observed during 7–8 April 2002 over the Korean peninsula.

2. Modeling of emitted particle size distribution

To improve the spectral dust emission estimated by Eq. (1), the concept of the minimally and fully dispersed parent soil particle size distribution is introduced. The particles size distribution is a weighted average of minimally ($p_m(d)$) and fully ($p_f(d)$) dispersed parent soil particle size distribution (Lu and Shao, 1999; Shao, 2001) and is given by

$$p_s(d) = \gamma p_m(d) + (1-\gamma) p_f(d), \tag{2}$$

where $p_s(d)$ is the suspended particle size distribution and γ the weighting factor. γ approaches to 1 for the weak erosion ($u_* \sim u_{*_t}$) and 0 for the strong erosion ($u_* \gg u_{*_t}$) where u_* is the friction velocity and u_{*_t} the threshold friction velocity. The weighting factor γ is estimated by

$$\gamma = \mathrm{e}^{-k(u_* - u_{*t})^n} \quad \text{if } (u_* \geqslant u_{*t}). \tag{3}$$

In this study, $k = 1$ and $n = 3$ are used (Lu and Shao, 1999; Shao et al., 2002). Both the minimally and fully dispersed particle size distribution for a given soil can be expressed as the sum of several log-normal distributions (Gomes et al., 1990; Chatenet et al., 1996; Shao, 2001) such that

$$p_m(d) = \frac{1}{d}\sum_{j=1}^{J} \frac{w_j}{\sqrt{2\pi}\sigma_j} \exp\left(-\frac{(\ln d - \ln D_j)^2}{2\sigma_j^2}\right), \tag{4}$$

where J is the number of modes, w_j the weight for the jth mode of the particle size distribution, D_j and σ_j parameters for the log-normal distribution of the jth mode. The nonlinear least-squares fitting technique can be used to determine the parameters w_j , D_j and σ_j from measured soil particle size distributions. Due to the lack of those parameters on the particle distribution in the Asian dust source region, we use soil samples collected in Australia by McTainsh (Shao et al., 2002). Table 1 shows the parameters for the log-normal distributions for minimally and fully dispersed particle size distributions for Sand, Loam, and Silty Clay (Shao et al., 2002) assuming soil texture being composed of a mixture of Sand, Loam and Silty Clay.

Eq. (4) is employed in the present numerical grid domain in the dust source region where the fractional coverage of soil types is classified (Park and In, 2003a, b; In and Park, 2002a). The log-normal distribution functions in Table 1 are averaged with the weighting factor of the fractional coverage of the soil type in each grid cell to estimate the spectral particle-mass concentration distribution in the source region. The soil textures at each source region are given in Table 2. The composition of the soil texture in Table 2 is approximated from 37 soil samplings taken in the Gobi, Sand, Loess and Mixed soil region in northern China (Park, 2002).

3. Used data and models

The 3 hourly WMO synoptic reporting data for the dust storms, dust rises and blowing dusts, the particle number concentration observed at Anmyondo and Seoul in Korea and the PM_{10} concentrations obtained

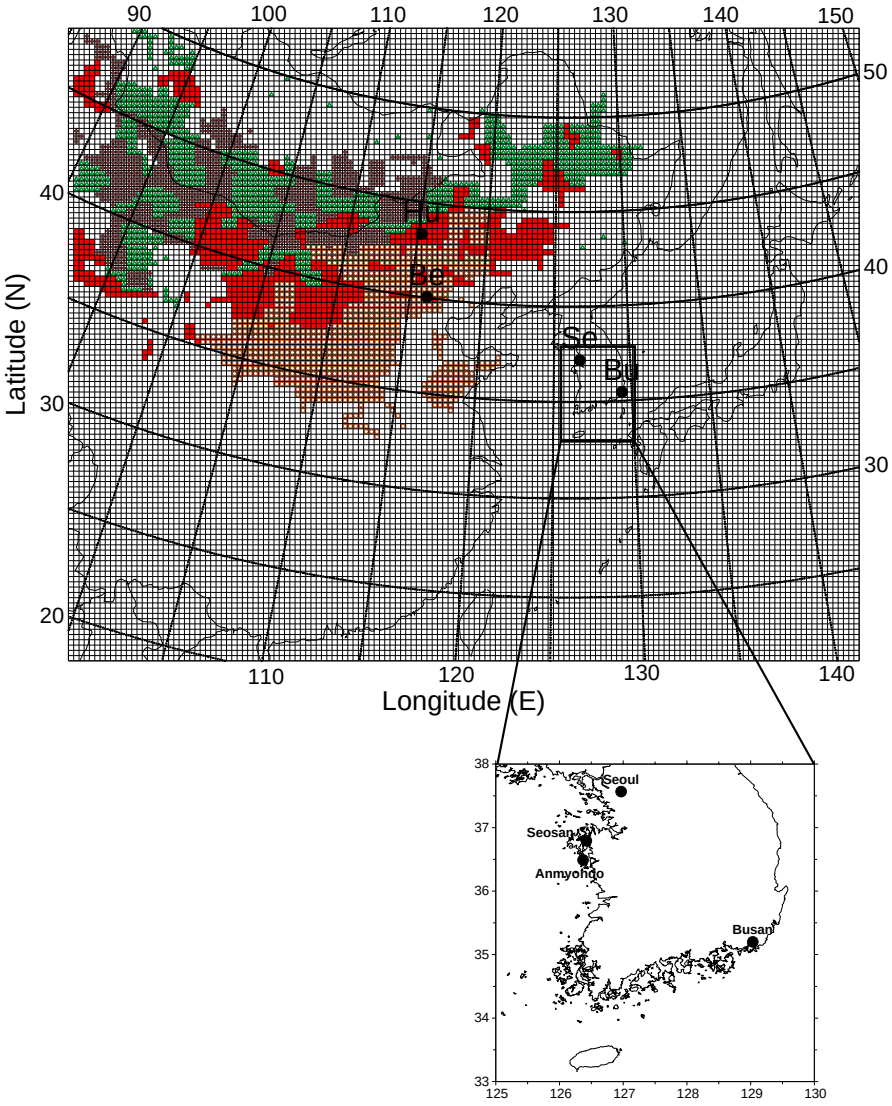

Fig. 1. The model domain with the indication of dust source regions (+ +) Gobi, (■ ■) Sand, (○ ○) Loess, and (△ △) Mixed soil and the enhanced map showing South Korea with locations of several air quality monitoring sites. The letters Hu, Be, Se and Bu represent Hunsendake, Beijing, Seoul and Busan, respectively.

from the monitoring sites in Korea (Fig. 1) and the aerosol index from the TOMS are used in this study for the period of 6–10 April 2002.

The Anmyondo site (Fig. 1) is a Background Air Pollution Monitoring Network site and monitors the greenhouse gases, air quality, and the chemical compositions of air. Spectral number concentrations of particles have been measured routinely in Seoul and Anmyondo (Fig. 1) simultaneously using an optical particle counter (OPC, HIAC/ROYCO 5230) since the spring of 1998 (Chun et al., 2001a, b). The particles ranging 0.3–25 μm are divided into eight size bins having eight cutoff diameters of 0.5, 0.82, 1.35, 2.23, 3.67, 6.06, 10 and 25 μm with the same log-scale interval.

The meteorological field data are obtained from the Regional Data Assimilation and Prediction System, that is, the operational meteorological model used in Korea Meteorological Administration (KMA). The aerosol model is exactly the same as in Park and In (2003a) except for the parameterization of the particle size distribution. The model domain and the dust source region delineated by four different soil types (Gobi, Sand, Loess, and Mixed soil) by Park and In (2003a) are shown in Fig. 1. Particles are divided into 10 bins

Table 1
Used parameters for the log-normal distribution to construct minimally ($p_m(d)$) and fully ($p_f(d)$) dispersed particle size distributions for Sand, Loam and Silty Clay (Shao et al., 2002)

Sample	Mode 1			Mode 2			Mode 3		
	w_1	$\ln(D_1)$	σ_1	w_2	$\ln(D_2)$	σ_2	w_3	$\ln(D_3)$	σ_3
$p_m(d)$									
Sand	0.0329	4.3733	0.8590	0.9671	5.7689	0.2526			
Loam	0.1114	4.3565	0.0257	0.4331	5.4092	1.0000	0.4554	5.1674	0.3824
Silty Clay	0.1070	4.4539	0.0236	0.3938	2.9319	1.0000	0.4991	4.5062	0.4473
$p_f(d)$									
Sand	0.0338	0.6931	1.0000	0.9662	5.6300	0.2542			
Loam	0.5844	4.6079	0.6141	0.3634	5.2050	0.2897	0.0522	7.0553	1.0000
Silty Clay	0.4452	0.6931	1.0000	0.3772	1.8900	0.8966	0.1776	5.6930	1.0000

Table 2
The composition of the soil texture at the four different soil types in the dust source region

Source region	Soil texture		
	Clay (%)	Loam (%)	Sand (%)
Gobi region	15	35	50
Sand region	10	10	80
Loess region	20	55	25
Mixed soil region	30	30	40

according to the division of OPC with additional two more bins for the larger particle than 25 μm in diameter with the maximum cutoff diameter of 74 μm in the model.

4. Synoptic features of the chosen Asian dust event

Fig. 2 shows the occurrence of dust storm (WMO reporting code of (S), S, S, |S, S, S, |S), dust rise ($) and suspended dust (S) reports at WMO synoptic stations on 00 and 12 UTC from 6 to 10 April 2002. The region of dust rise well coincided with the region of the prevailing strong wind exceeding 10 m s^{-1} in association with a developing low-pressure system (not shown here) in the arid inland region of China as in In and Park (2002b). On 6 April, the main reporting regions of dust storms and blowing dusts were Mongolia, Inner-Mongolia Plateau and Loess region. They moved progressively eastward in association with the movement of the weather system. Suspended dusts were reported in the Shandong Peninsula and North East China on 7 April. On 8 April, blowing dust occurred continuously in the Loess region. Dust storms and suspended dusts appeared in the whole Korean Peninsula and Jilin province in China. After 8 April, dust storms and blowing dusts ended in the source region. However, suspended dusts continuously reported in South Korea and southern Japan. Spatial distribution of aerosol index obtained from the TOMS clearly showed the pathway of the dust storm originated in the Inner-Mongolia Plateau on 6 April 2002 (Fig. 3).

PM_{10} concentrations observed at several monitoring sites in South Korea (Fig. 4) started to increase on 7–8 April. First peak concentrations in Seoul and Seosan (Figs. 4c and d) were more than 1500 μg m^{-3} and the second peaks in Seoul and Seosan exceeded 1000 and 900 μg m^{-3}, respectively. The observed PM_{10} concentration in Korea started to increase from north and gradually moved southeastward with decreasing intensity. The center of the dust cloud passed over the northern part of Korea. Consequently, Busan (Fig. 4e) had relatively lower dust concentration. After 10 April, the dust concentrations have slowly decreased to a background concentration at most sites in Korea.

5. Results and discussion

5.1. Spatial and temporal evolution of the simulated dust concentration

The spatial distributions of the vertically integrated dust concentration are shown in Fig. 5. A significant amount of dust emission occurs near the Mongolia and Inner-Mongolia border on 6 April. This is also seen in the TOMS aerosol index (Fig. 3b). Thereafter, the dust cloud rapidly expends eastward and southward in association with the vigorous emissions in the source regions. Very strong westerlies to northwesterlies carry the dust cloud downstream continuously resulting in a dust front stretching from southwest to northeast similar to a cyclonic vortex until 8 April. Consequently, the dust cloud covers over North Korea, northern North East

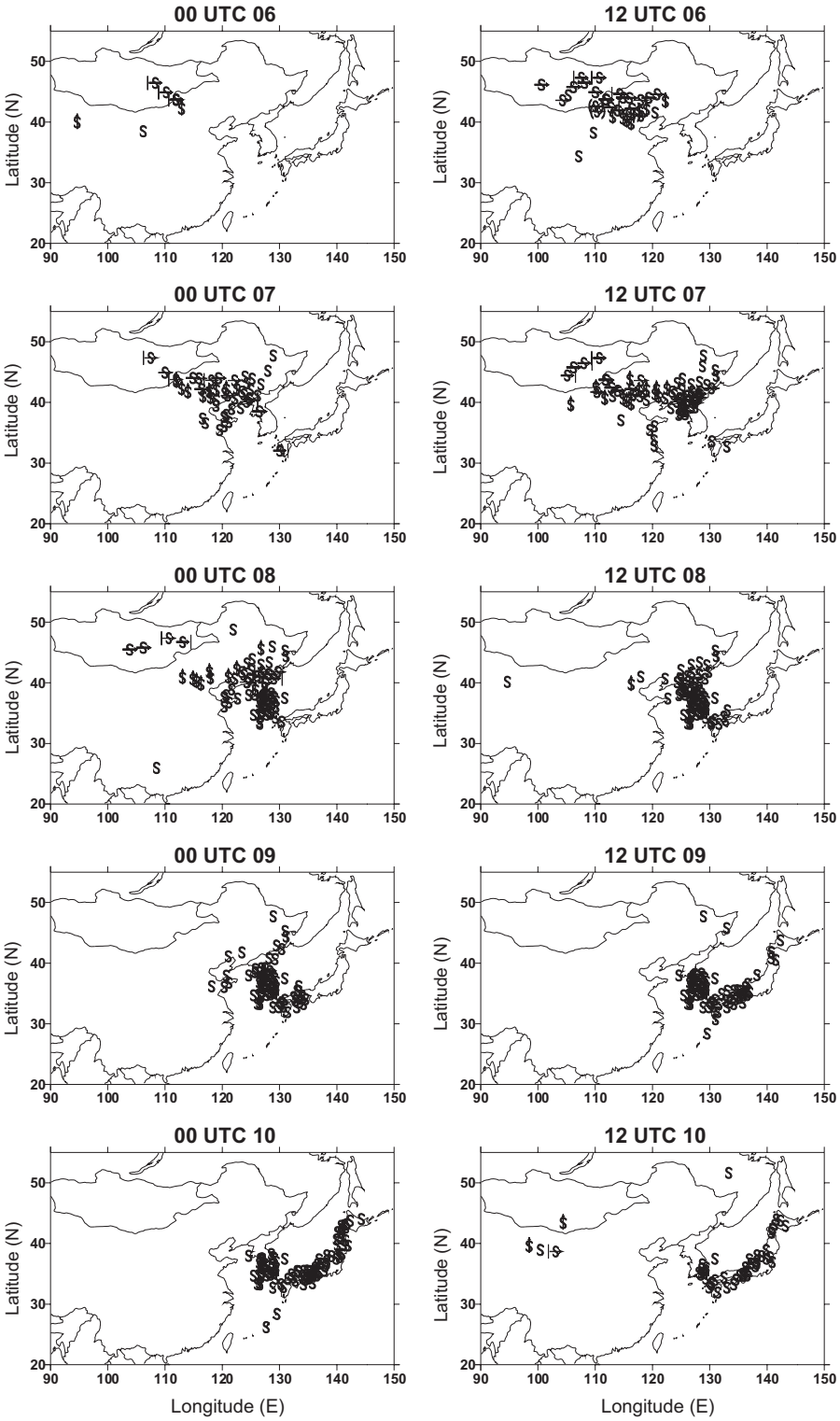

Fig. 2. Spatial distributions of dust-rise ($), dust storm ((S), S, S, |S, S|, S, |S) and Yellow Sand (S) reporting sites from 6 to 10 April 2002 in a 12-h interval.

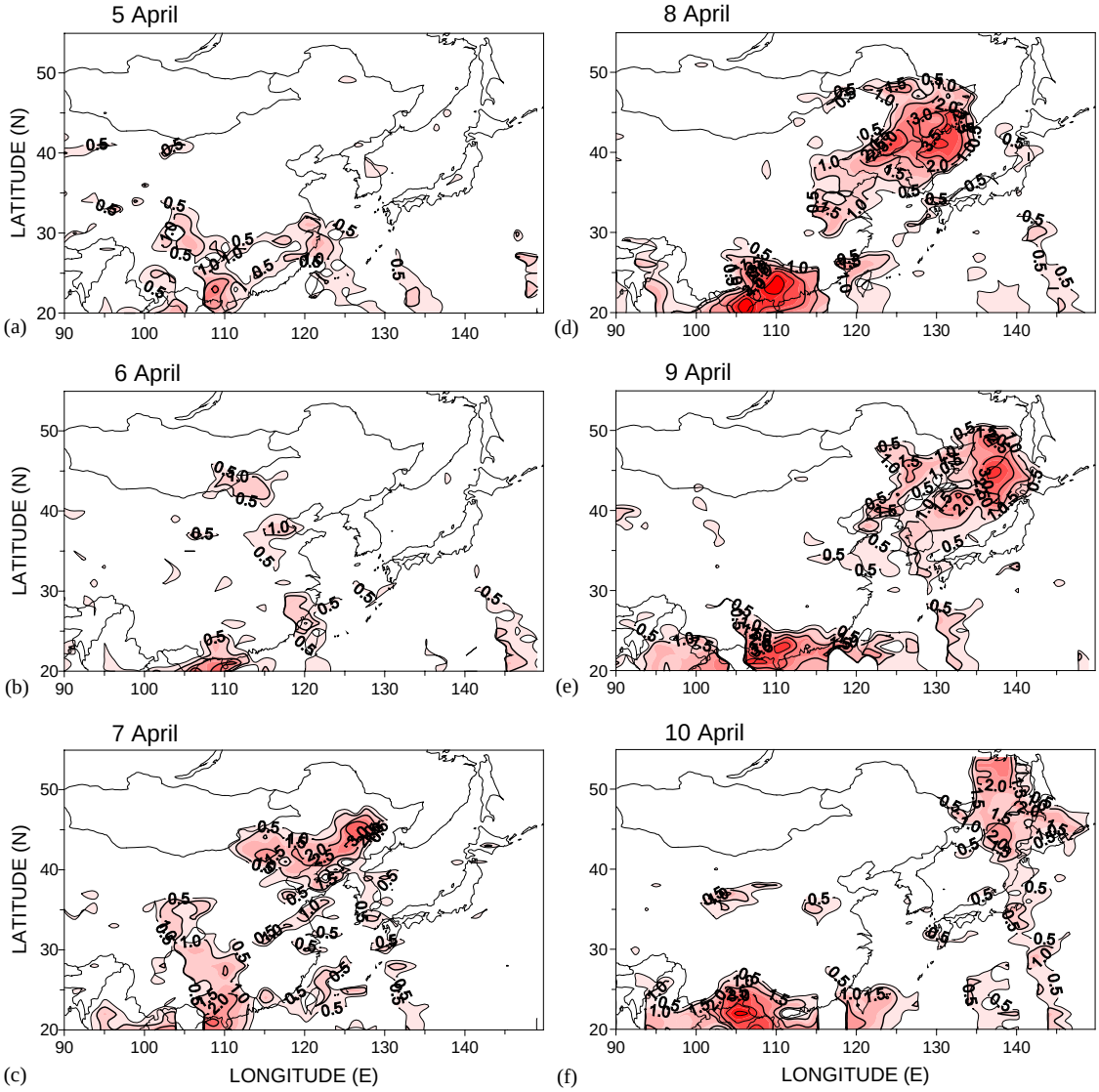

Fig. 3. Time evolution of the spatial distribution of aerosol index obtained by TOMS on (a) 5, (b) 6, (c) 7, (d) 8, (e) 9, and (f) 10 April 2003.

China and the eastern border of Russia and China. Meanwhile, dusts emitted in the Sand and Loess region of northeastern China are added to the pre-existing dust layer, yielding a more denser dust layer that is elongated from southern China to North East China. Thereafter, the dust-laden air moves southward to South Korea on 8–9 April. After 9 April, the dust layer is transported eastward over South Korea, the East Sea, and Hokkaido of Japan. The spatial distribution pattern of the simulated dust cloud resembles quite well to that of TOMS aerosol index (Fig. 3). This can be seen more easily if we compare the isoline of $10^7\,\mu g\,m^{-2}$ of the simulated dust cloud in Fig. 5 with the TOMS aerosol index isoline of 0.5 in Fig. 3. The slight difference might be associated with the time difference between the satellite scanning time and the model representing time. However, the present model does not take into account the high aerosol index region in southern China appeared in the TOMS aerosol index (Fig. 3). This is not associated with Yellow Sand observed in Korea.

The time series of modeled PM_{10} concentrations averaged for the layers of below 100, 100–1500 and above 1500 m from the ground are also shown in Fig. 4. The model simulates quite well the observed surface concentrations at Seoul (Fig. 4c) and Seosan (Fig. 4b) and the starting and ending times of the dust storm. However, the simulated concentration at Busan which is

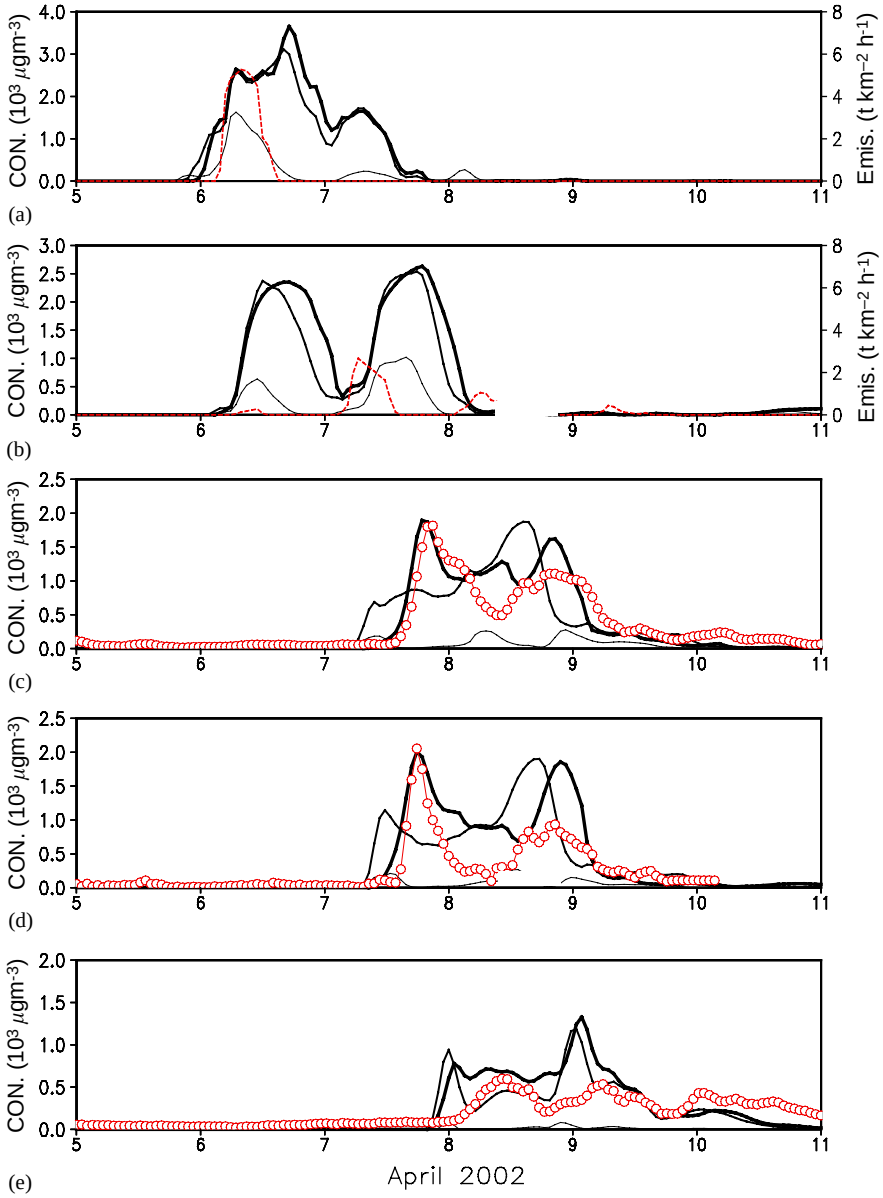

Fig. 4. Time series of modeled mean PM_{10} concentration ($\times 1000\,\mu g\,m^{-3}$) averaged for the layers of surface to 100 m (▬▬), 100–1500 m (——), above 1500 m (—) with the emission rates (– – – –, $t\,km^{-2}\,h^{-1}$) and observed surface PM_{10} concentration (-○-○-○-) at (a) Hunsendake, (b) Beijing, (c) Seoul, (d) Seosan, and (e) Busan.

located at the southeastern fringe of the Korean peninsula is a little lower than the observed one since the simulated main dust storm has passed through northern Korea. There are two peaks in both the modeled and observed concentrations with a maximum at the first peak. Dust concentrations tend to increase in the middle layer (100–1500 m layer) first rather than in the lowest layer away from the source regions (Fig. 4). The simulated first peak has higher concentration than the second peak at Seoul and Seosan, whereas the second peak has higher concentration in the middle layer than in the lowest layer suggesting two different pathways of these dust storms. Busan shows quite different temporal distribution pattern compared with that at Seoul and Seosan. The peak concentrations in the middle and lower layers occur simultaneously with nearly same PM_{10} concentration. This might be attributed to the discrepancies in simulated meteorological fields. The PM_{10} concentration above 1500 m is very low in all sites.

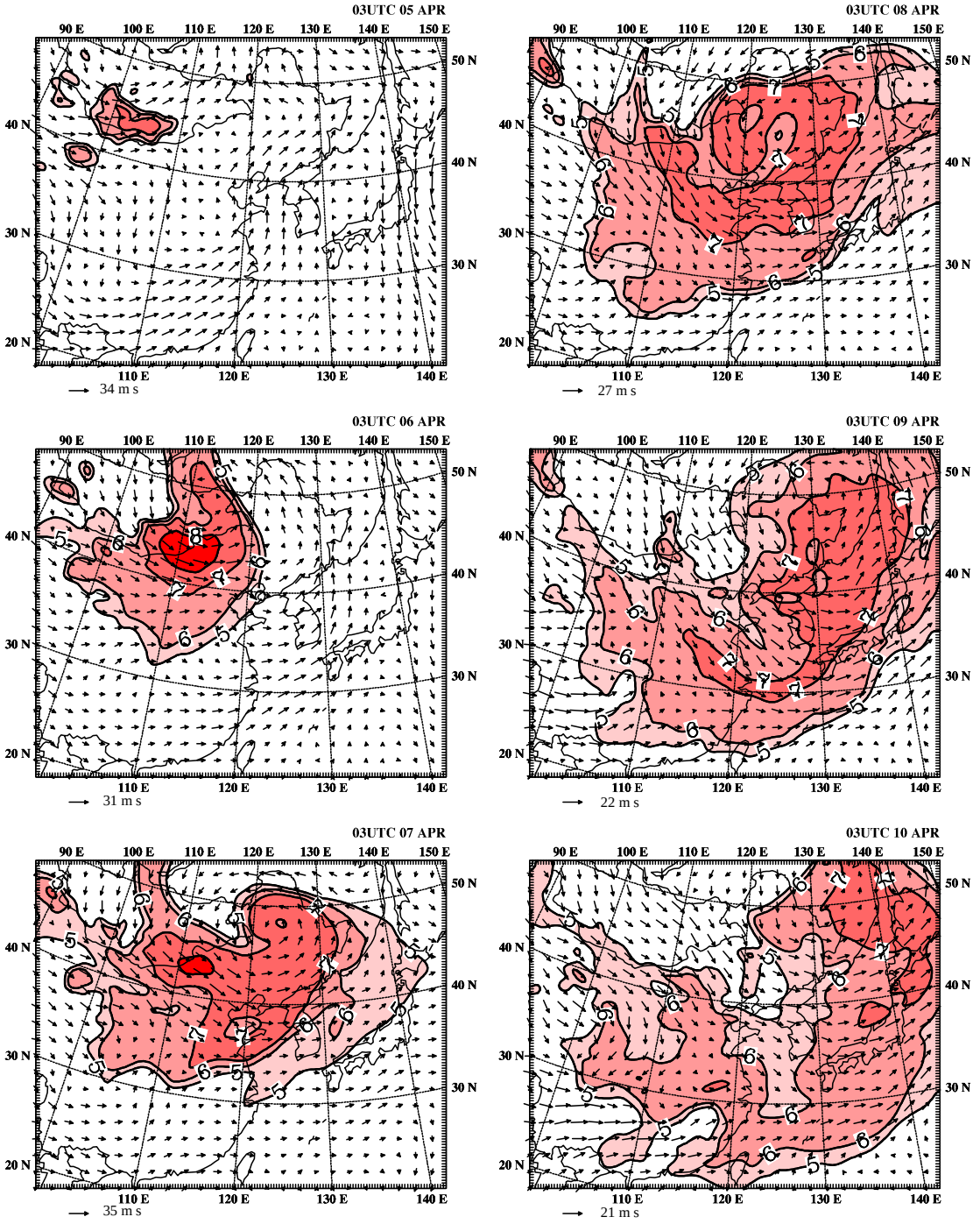

Fig. 5. Spatial distribution of the modeled vertically integrated TSP concentration expressed in common logarithm ($\mu g\,m^{-2}$) with the wind vector at the height of 1500 m.

The model simulates quite well the starting, ending, and dust peak appearing times of the Yellow Sand event observed in Korea. The model also reproduces quite well the maximum PM_{10} concentration.

5.2. Dust particle size distribution

The particle number concentration measured by the OPC in Seoul and Anmyondo shows an abrupt

increase in 0.82–6.06 μm particles during the dust period (Figs. 6a and b). There are two episodes of the dust transport during the period of 7–9 April. The first one has stronger intensity than the second one as already seen in Fig. 4. The concentration in the smallest particle size (0.3–0.5 μm) decreases remarkably during the dust period but increases after the dust period in Seoul (Fig 6a). These features were also observed for the case of April 1998 (Chun et al., 2001a). This might be associated with the reduction of smaller particles due to collision by larger particles. However, at Anmyondo, that is, a background monitoring site, all particle sizes ranging from 0.3 to 25 μm have increased significantly during the Yellow Sand period (Fig. 6b).

During the Asian dust event in April 1998, the total concentration of aerosols greater than 2.23 μm was substantially increased by approximately one order of magnitude compared to the non-dust event period at Seoul and Anmyondo (Chun et al., 2001a). However, the particles smaller than 1 μm reduced significantly during the heavy dust period in the urban area of Seoul. It is worthwhile to note that the number concentration of the smallest particles decreases significantly in the urban area (Fig. 6a) whereas it increases remarkably at the background site (Fig. 6b) during the dust storm period. Some chemical analyses of these particles are required to understand these phenomena.

Fig. 7 presents time series of the converted PM_{10} mass concentrations from the observed number concentration at Anmyondo assuming a spherical shape of a particle with a constant density of 2600 kg m^{-3} (Park and In, 2003a) and the observed PM_{10} concentration at Seosan which is the nearest air monitoring site to Anmyondo (Fig. 1). The converted mass concentration and observed concentration show a slight time difference due to the distance between these two sites; however, the time variation patterns of these two concentrations are quite similar.

Comparisons of the modeled and converted spectral-mass concentration distribution are shown in Fig. 8. Fig. 8a shows the result of the spectral-mass concentration estimated by using Eq. (1) at Hunsendake and Anmyondo. The spectral number concentration measured at Anmyondo is averaged for 12 h during the period of high dust concentration. The averaged spectral number concentration is converted to the spectral-mass concentration using the constant density of 2600 kg m^{-3}. The simulated and the converted spectral-mass concentration for the same time period at Anmyondo are also shown in Fig. 8a. The simulated spectral dust concentration using Eq. (1) shows quite different from that of the observation (Fig. 8a). The measured mass

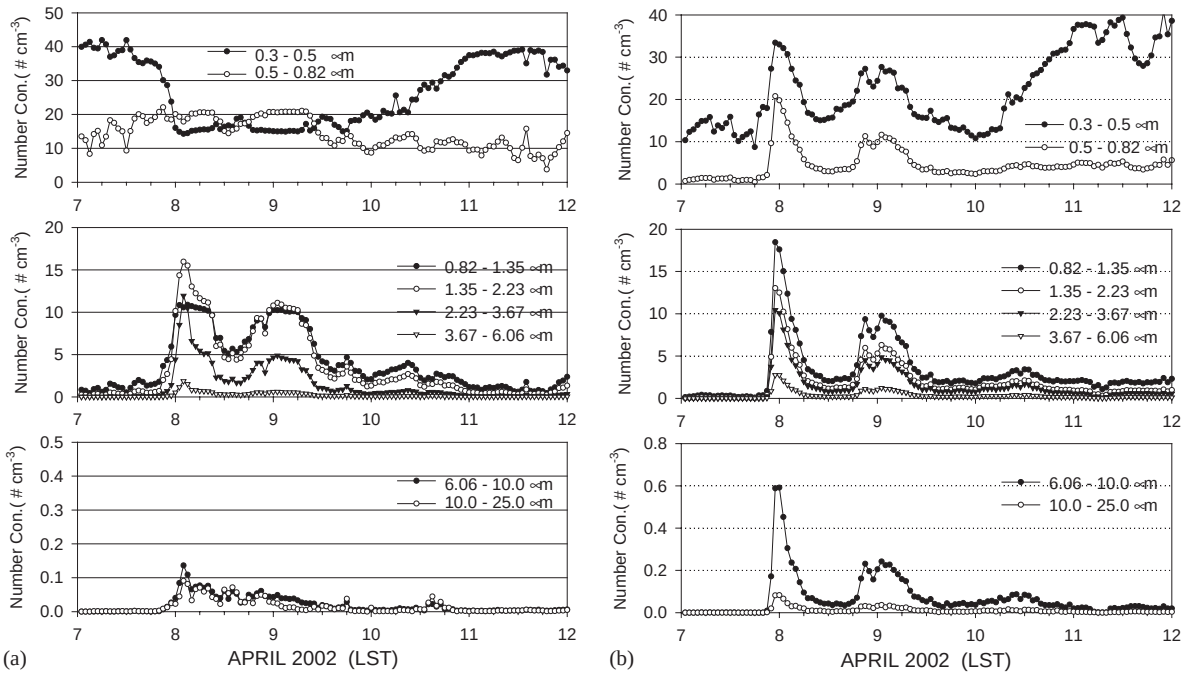

Fig. 6. (a) Time series of particle number concentrations for 7–11 April 2002 observed at Seoul, and (b) same as in Fig. 6a except for Anmyondo.

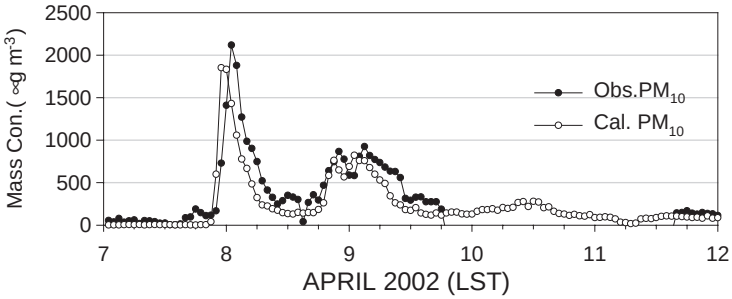

Fig. 7. Temporal variations of the mass concentrations of PM_{10} converted from the observed number concentration at Anmyondo (-○-○-○-) and observed PM_{10} concentration at Seosan (-●-●-●-) from 7 to 11 April 2002.

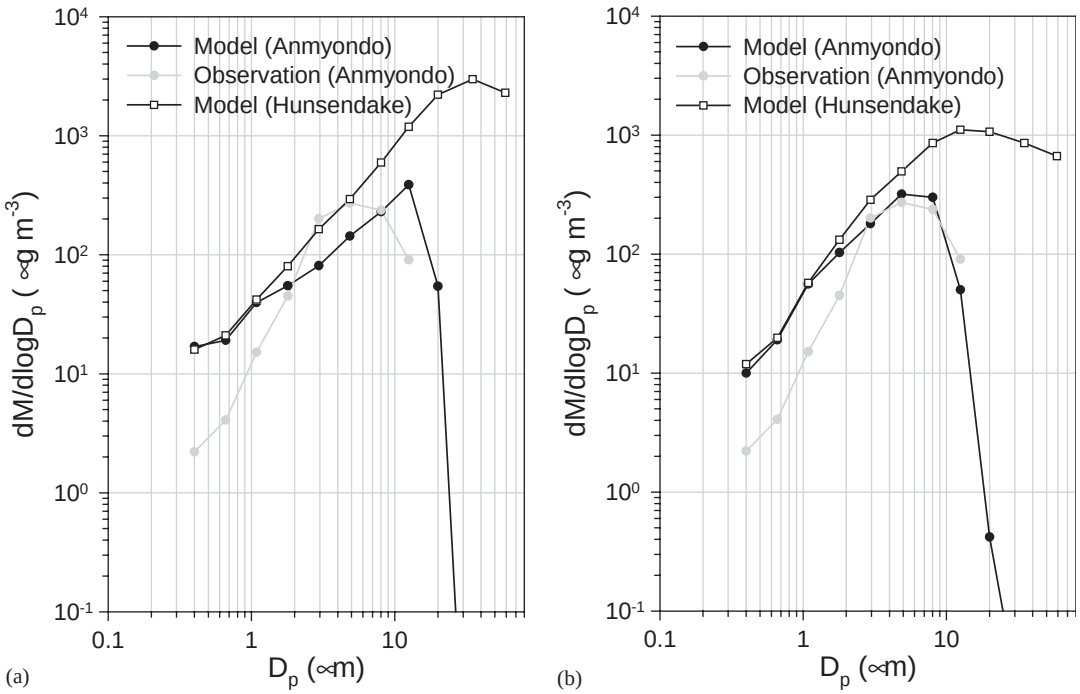

Fig. 8. Modeled spectral-mass concentration distributions estimated by using (a) 1.5 power law of the particle radius, and (b) the sum of three log-normal distributions of soil particle sizes at Hunsendake (-□-□-□-) and Anmyondo (-●-●-●-) with the spectral-mass concentration converted from the observed number concentration (-●-●-).

concentration has a significantly high concentration in the range of 2–8 μm but a remarkably low concentration below 2 μm in diameter compared with that of the model (Fig. 8a). Consequently, this results in a good agreement between the observed and modeled PM_{10} concentration (Fig. 5c).

The spectral-mass concentration estimated by Eq. (4) (the particle size distribution expressed as the sum of several log-normal distributions) yields more reasonable spectral-mass concentration than that estimated by Eq. (1) even though detailed soil parameters are not used (Fig. 8b). This clearly suggests that much improved spectral-mass concentration can be obtained with the sum of several log-normal distributions of particle sizes in the source regions. This implies that particle size distributions of Yellow Sand are consistent with those found in the USA (Patterson and Gillette, 1977a, b), Central Asia (Sviridenkov et al., 1993) and the Sahara desert (Gillette et al., 1997). However, much improved spectral-mass concentration requires detailed information on soil textures and soil particle distributions in the source regions.

6. Summary and conclusions

There were large dust rises on 6–8 April in the source regions of inland China especially in Inner-Mongolia and Loess region in East China. The dust transport to Korean peninsula takes about 1 day (Fig. 4). Consequently, the observed dust concentration in the Korean peninsula is extremely high during the dust storm period. The spatial distribution of vertically integrated dust concentration obtained by the model quite well coincides with that of aerosol index obtained by TOMS (Fig. 3). The model also simulates quite well the starting, ending, dust peak appearing time and the maximum PM_{10} concentration compared with those observed in South Korea (Fig. 4). During the Yellow Sand period from 7 to 9 April 2002, number concentration of particles at Seoul and Anmyondo has increased substantially in the size range of about 1–10 μm in the Korean peninsula.

The minimally and fully dispersed particle size distributions as the sum of three log-normal distributions of soil textures (Eq. (4)) that are consistent with those found in the USA, Central Asia and the Sahara desert are found to yield more reasonable spectral-mass concentration distribution than that obtained by the 1.5 power law of the spectral dust emission flux in the source region especially in the size range of larger than 10 μm. However, the PM_{10} mass concentration distribution over South Korea is not significantly changed.

Further studies on the emission parameterization are required on the basis of observed soil particle size distribution in the source regions to estimate more accurate long-range transported spectral-mass concentration at the distant regions. This is now on hand.

Acknowledgements

This research was supported partially by the Korea Meteorological Administration (KMA), Korea Science and Engineering Foundation (KOSEF) and the Climate Environmental System Research Center in Seoul National University. OPC data are provided by the Background Monitoring Station at Anmyondo. Special recognition goes to two anonymous reviewers for their helpful comments.

References

Bai, N., Zhang, K., 2001. About Sandstorms in China, 2000–2001. Proceedings of the Seventh International Joint Seminar on the Regional Deposition Processes in the Atmosphere, Tsukuba, Japan, 20–22 November.

Chatenet, B., Marticorena, B., Gomes, L., Bergametti, G., 1996. Assessing the microped size distributions of desert soils erodible by wind. Sedimentology 43, 901–911.

Chun, Y.-S., Kim, J., Choi, J.C., Boo, K.O., Oh, S.N., Lee, M., 2001a. Characteristic number size distribution of aerosol during Asian dust period in Korea. Atmospheric Environment 35, 2715–2721.

Chun, Y.-S., Boo, K.O., Kim, J., Park, S.-U., Lee, M., 2001b. Synopsis, transport, and physical characteristics of Asian dust in Korea. Journal of Geophysical Research 106, 18461–18469.

Gillette, D.A., 1981. Production of dust that maybe carried great distances. Special Paper on Geological Society of America 186, 11–26.

Gillette, D.A., Fryrear, D.W., Gill, T.W., Ley, T., Cahill, T.A., Gearhart, E.A., 1997. Relation of vertical flux of particles smaller than 10 μm to total Aeolian horizontal mass flux at Owens Lake. Journal of Geophysical Research 102 (D22), 26009–26016.

Gomes, L., Bergametti, G., Dulac, F., Ezat, U., 1990. Assessing the actual size distribution of atmospheric aerosols collected with a cascade impactor. Journal of Aerosol Science 21, 47–59.

In, H.-J., Park, S.-U., 2002a. A simulation of long-range transport of Yellow Sand observed in April 1998 in Korea. Atmospheric Environment 36, 4173–4187.

In, H.-J., Park, S.-U., 2002b. Long-range transport of Asian dust (Yellow Sand) event observed in April 2002. Proceeding of the Eighth International Joint Seminar on Regional Deposition Processes in the Atmosphere, Irktusk, Russia.

Lu, H., Shao, Y., 1999. A new model for dust emission by saltation bombardment. Journal of Geophysical Research 104, 16827–16842.

Park, S.-U., 2002. Field survey of Yellow Sand source regions. Proceedings of the Workshop of Asian dust, 22 March 2002, Korea meteorological Administration, Korea.

Park, S.-U., In, H.-J., 2003a. Parameterization of dust emission for the simulation of the Yellow Sand (Asian dust) observed in March 2002 in Korea. Journal of Geophysical Research, in press.

Park, S.-U., In, H.-J., 2003b. A numerical simulation of the Yellow Sand event observed in March 2002 in Korea with statistically derived dust emission parameterizations. Proceeding of the Second Workshop of Air quality Modeling Challenges, Tsukuba, Japan.

Patterson, E.M., Gillette, D.A., 1977a. Measurements of visibility vs. mass-concentration for airborne soil particles. Atmospheric Environment 11, 193–196.

Patterson, E.M., Gillette, D.A., 1977b. Commonalities in measured size distributions for aerosols having a soil derived component. Journal of Geophysical Research 82, 2074–2082.

Shao, Y., 2001. A model of mineral dust emission. Journal of Geophysical Research 106, 20239–20254.

Shao, Y., Jung, E., Leslie, L.M., 2002. Numerical prediction of northeast Asian dust storms using an integrated wind erosion modeling system. Journal of Geophysical Research 107 (D24), 4814 doi:10.1029/2001JD001493.

Sviridenkov, V., Gillette, D.A., Isakov, A., Sokolik, I.N., Smirnov, V.V., Balan, B.D., Panchenko, M.V., Andronova, A.V., Kolomiets, S.M., Zhukovsky, D.A., 1993. Microphysical

characteristics of dust aerosol measured during the Soviet–American experiment in Tadzhikistan, 1989. Atmospheric Environment 27a, 2481–2486.

Westphal, D.L., Toon, O.B., Carlson, T.N., 1987. A two-dimensional Investigation of the dynamics and microphysics of Saharan dust storms. Journal of Geophysical Research 92, 3027–3049.

Westphal, D.L., Toon, O.B., Carlson, T.N., 1988. A case study of mobilization and transport of Saharan dust. Journal of Atmospheric Sciences 45, 2145–2175.